Short-Crack *T*-Curves and Damage Tolerance in Alumina-Based Composites

L.M. Braun, S.J. Bennison and B.R. Lawn

Composites and Advanced Ceramic Materials
American Ceramic Society, Ohio
Vol. **13**, p. 156, 1992.

SHORT-CRACK *T*-CURVES AND DAMAGE TOLERANCE IN ALUMINA-BASED COMPOSITES

Linda M. Braun, Stephen J. Bennison & Brian R. Lawn, Materials Science and Engineering Laboratory, National Institute of Standards & Technology, Gaithersburg, MD 20899

ABSTRACT

A procedure for evaluating short-crack toughness curves (*T*-curves) from quantitative *in situ* observations of Vickers indentation cracks during stressing is described. We demonstrate the procedure with results on an Al_2O_3–Al_2TiO_5 composite with strong *T*-curve behavior and attendant crack stabilization from grain-localized-crack-bridging. The stabilization allows the material to tolerate multiple damage accumulation during loading.

INTRODUCTION

Rising toughness with crack extension (*T*-curve or *R*-Curve) underlies the mechanical properties of many ceramic materials [1-5]. Two issues are central to optimizing the *T*-curve characteristics for structural applications. The first involves identification and manipulation of the microstructural parameters that control the *T*-curve. The second involves evaluation of the *T*-curve in the "short-crack" domain, i.e. on a scale comparable to the microstructure. The short-crack *T*-curve controls the strength [1,5,6], flaw sensitivity [1,5,6], and reliability [5] of ceramics and is, therefore, highly pertinent to engineering design.

In this paper we present a strategy for improving the *T*-curve properties of Al_2O_3-based ceramics through enhancement of residual thermal expansion (TEA) mismatch stresses via incorporation of a second phase, β-Al_2TiO_5. These stresses augment the frictional grain-bridging mechanism responsible for the *T*-curves and associated flaw tolerance in Al_2O_3 (and many other nontransforming) ceramics [7-9]. We describe a procedure for evaluating the short-crack *T*-curve from quantitative *in situ* observations of Vickers indentation cracks during stressing [10], in conjunction with indentation–strength data [9], on the tailored Al_2O_3–Al_2TiO_5 composite.

EXPERIMENTAL

The Al_2O_3–Al_2TiO_5 composite was fabricated by pressureless sintering [8]. A colloidal suspension of high purity powders (α-Al_2O_3, Sumitomo AKP-HP grade, 99.995% pure, 0.5 μm crystallites; β-Al_2TiO_5, Trans-Tech., 99.9% pure, 1-5 μm crystallites) in water (pH ~3) was dried and formed into green disks by single-end die pressing (63 MPa) in high-purity graphite followed by wet-bag isostatic pressing (350 MPa). The disks were calcined in air at 1050°C for 12 hr and sintered at 1600°C for 1 hr. The density was measured using the Archimedes method [11], and grain size using a linear intercept technique [12] on thermally etched (1490°C, 6 min. air) polished sections.

The short-crack *T*-curve characteristic of the composite was determined from quantitative observations of crack growth from a Vickers indentation during loading [6,13-15]. This was accomplished using a custom-made biaxial stressing fixture, punch (diam 6mm) on six-ball support (diam 23mm). A force was applied using a piezoelectric translator and measured using a strain gage load cell. The fixture could be placed on an inverted optical microscope with long working-distance lenses, or in a scanning electron microscope (SEM). Crack evolution and crack-microstructure interactions were taped on a video cassette recorder. The experimental procedure consisted of: (i) indenting the center of a polished disk (diam 30mm, thickness 4mm) at a specified peak contact load (20-300 N); (ii) covering the indentation site with a drop of dry silicone oil and a glass cover slide for optical imaging; (iii) loading the specimen and simultaneously recording the applied stress (calculated from the force and geometry using thin-plate formulas) and crack growth during evolution to failure; (iv) measuring the crack lengths at jump and arrest points during loading directly from the video tape.

Indentation-strength tests were carried out using a universal testing machine, to determine the flaw tolerance characteristics. Vickers indentations at specified loads were made in the center of each polished specimen (diam 20mm, thickness 3mm). The disks were broken in biaxial flexure using a punch (diam 4mm) on three-ball support (diam 15mm). These tests were conducted with a drop of dry silicone oil on the indentation site and broken in fast loading (<10 ms) to maintain "inert" conditions. Post-mortem examinations were made of all broken specimens to confirm failure initiation from the indentation sites. A minimum of 4 specimens per contact load were fractured. Comparative *in situ* and strength tests were also carried out on a control fine-grain (6 μm) Al_2O_3.

RESULTS

Figure 1 shows the microstructure of the Al_2O_3–Al_2TiO_5 (20 vol.%) composite. The microstructure has a density >99% and a matrix grain size of 6 μm. The grain structure is equiaxed with the Al_2TiO_5 particles distributed mainly at the matrix grain boundaries, with occasional clusters of 5-10 particles. These clusters are probably remnant agglomerates from the starting powder.

The indentation crack patterns in the composite were well formed at all indentation loads. During stressing both of the mutually orthogonal radial crack systems were observed to extend stably, with discrete jumps. At approximately 80% of the failure stress one set of radial cracks began to extend at the expense of the other. The total extension of this dominant set relative to the initial crack length exceeded the factor 2.5 characteristic of indentation flaws in materials with single-valued toughness. Such enhanced extension indicates the presence of an additional stabilizing contribution (i.e. above and beyond that of the residual contact field) to the crack-tip *K*-field [1,5,16], consistent with a rising *T*-curve.

The *in situ* testing fixture also facilitated detailed observations of crack-microstructure interactions in the SEM. Examinations of extended cracks during loading to failure revealed evidence for copious grain-interlock bridging at crack interfaces. Figure 2 indicates that the Al_2TiO_5 particles play a highly active role in the bridging process responsible for the strong *T*-curve in this material [5,7,9].

The stabilization imparted by the *T*-curve is strong enough to allow the development of multiple macro-crack systems from natural flaws in the tensile surface of the specimen. Figure 3, an optical micrograph recorded at slight overfocus, reveals the presence of general damage in the form of multiple "macro-cracks", i.e. cracks typically 30-300 grain diameters in length. The incidence of these cracks corresponded to a significant nonlinearity in the measured load-deflection curve in this material [8]; interactions with the macro-crack damage therefore influences the strength and damage tolerance characteristics. Failure of the specimen nevertheless still occurred from the indentation cracks. In unindented specimens, strength is controlled by percolation of the macro-cracks.

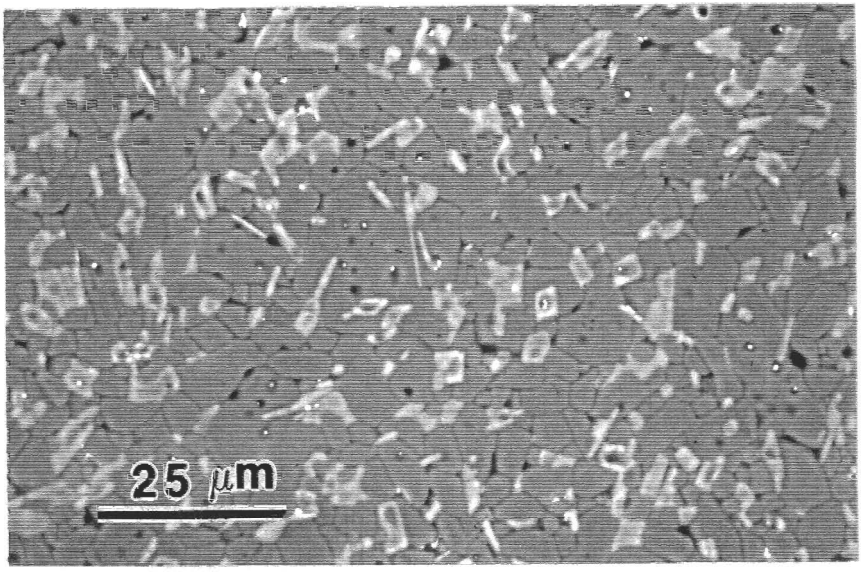

Figure 1 SEM micrograph (backscattered) of the Al_2O_3–Al_2TiO_5 (20 vol.%) composite. White phase Al_2TiO_5; grey phase Al_2O_3; black phase porosity.

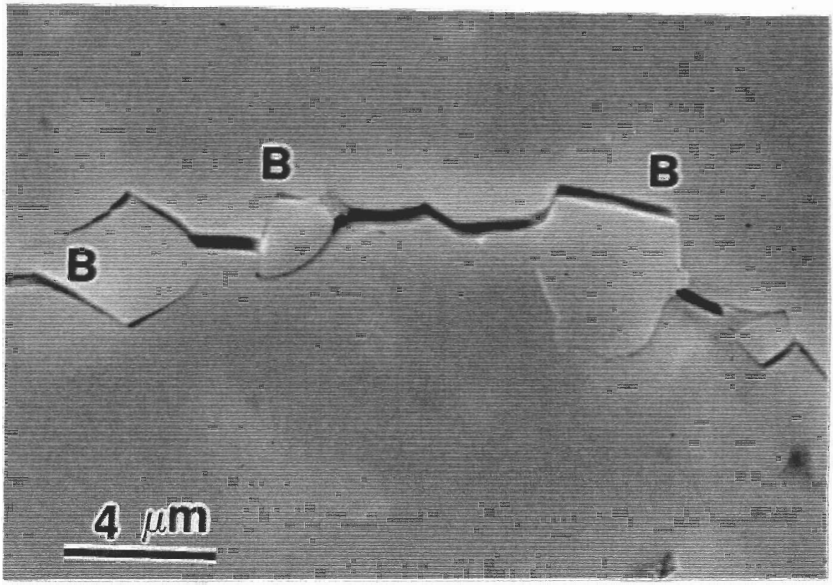

Figure 2 SEM micrograph (backscattered electrons) of a loaded indentation crack showing bridging in Al_2O_3–Al_2TiO_5 composite. B marks grain-grain bridge sites.

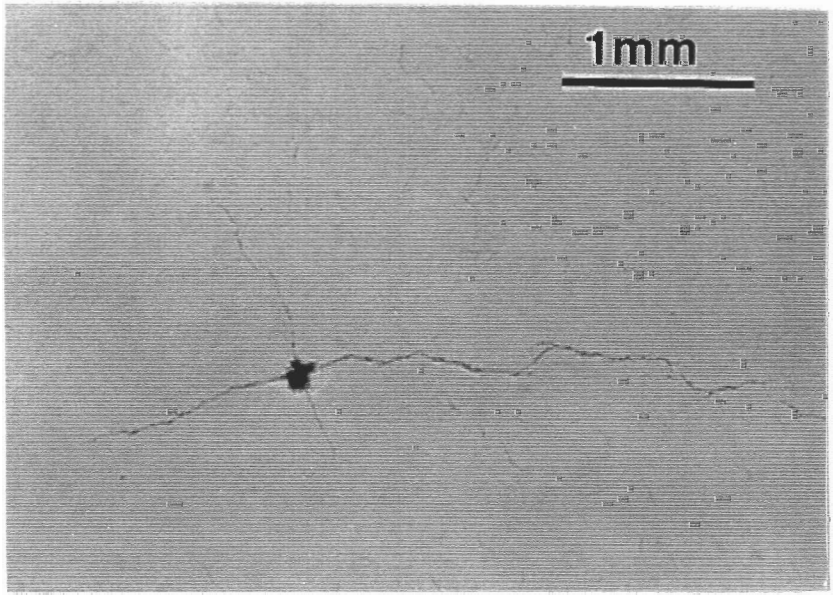

Figure 3 Optical micrograph (bright field) of damage in Al_2O_3–Al_2TiO_5 composite. Multiple cracks are present and stable during loading. The image is deliberately overfocused to enhance contrast.

T-CURVE ANALYSIS AND STRENGTH

The *T*-curve is determined from the stress-intensity field governing growth of indentation cracks subject to microstructural closure forces. The crack-tip *K*-field, K_*, as a function of radial crack size c is [1,5-7]

$$K_*(c) = K_A + K_R + K_\mu$$

$$= \psi\sigma_A c^{1/2} + \chi P/c^{3/2} + K_\mu(c) = T_0 \qquad (1)$$

at equilibrium. K_A is the stress-intensity factor associated with the applied stress field σ_A, K_R with the residual contact field at an indentation load P, and K_μ with microstructural shielding (the source of the *T*-curve); $\psi = 0.75$ [10] is a geometrical coefficient that characterizes the half-penny-like crack configuration, and $\chi = 0.076$ [10] is a coefficient that characterizes the intensity of the residual contact field; T_0 is the intrinsic material toughness, governed by the grain boundary fracture energy for intergranular fracture. Eqn. 1 may be transposed into a form appropriate to a "global" (i.e. externally measured) *K*-field

$$K_A'(c) = \psi\sigma_A c^{1/2} + \chi P/c^{3/2}$$

$$= T_0 - K_\mu(c) = T_0 + T_\mu(c) = T(c) \qquad (2)$$

where $K_A'(c)$ is an effective applied stress-intensity factor, $T_\mu(c) = -K_\mu(c)$ is a shielding toughness term, and $T(c)$ defines the *T*-curve. Measurements of σ_A and c at given load P are substituted into Eqn. 2 to evaluate $T(c)$.

A quantitative evaluation of the short-crack *T*-curve for our composite material is accordingly presented in fig. 4. The $\sigma_A(c)$ data used in this evaluation were taken before the onset of nonlinear load-deflection behavior. The toughness increases monotonically from $T \approx 1.8$ MPa.m$^{1/2}$ at $c \approx 100$ μm to $T \approx$ MPa.m$^{1/2}$ at c ≈ 2 mm. The maximum measured toughness does not achieve the steady-state value $T \approx 9$ MPa.m$^{1/2}$ estimated from long-crack (disk-compact-tension geometry) measurements [17]. Note that the initial toughness falls below the intrinsic toughness for a fine-grain control Al_2O_3, $T_0 = 2.75$ MPa.m$^{1/2}$ [7,18]. At very small crack sizes local residual tensile TEA stresses *drive* crack growth ($T < T_0$); at large crack sizes, closure stresses from bridging dominate, and *inhibit* growth ($T > T_0$).

The pronounced crack stabilization imparted by the strong *T*-curve in the Al_2O_3–Al_2TiO_5 composite is evident in the indentation-strength response shown in fig. 5. The strength of the composite is relatively insensitive to indentation load, and shows a marked deviation from the ideal $P^{-1/3}$ behavior for the control Al_2O_3 [6,16,18]. In contrast to the composite, the control material is highly flaw-sensitive, with relatively low strengths in the domain of intermediate cracks (high indentation loads).

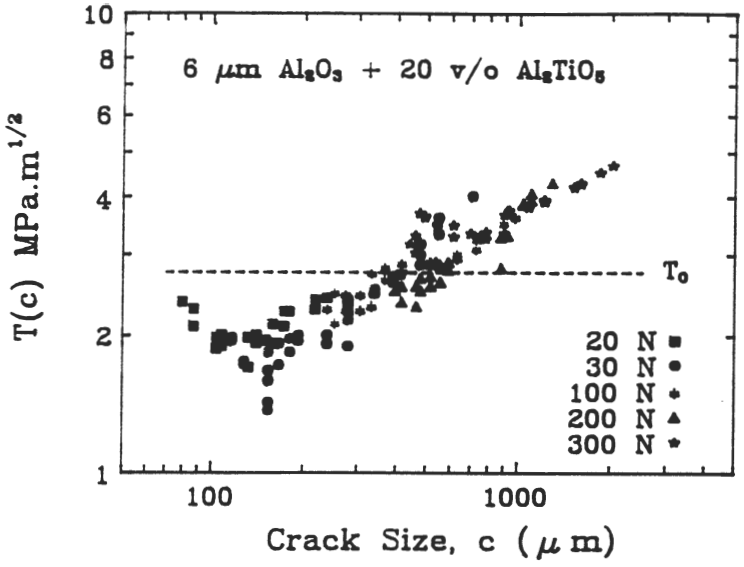

Figure 4 T-curve of Al_2O_3–Al_2TiO_5 composite as evaluated by *in situ* observations of Vickers indentation cracks (P = 20, 30, 100, 200, 300N) during loading. The baseline toughness T_0 = 2.75 MPa.m$^{1/2}$ is for fine-grain control Al_2O_3.

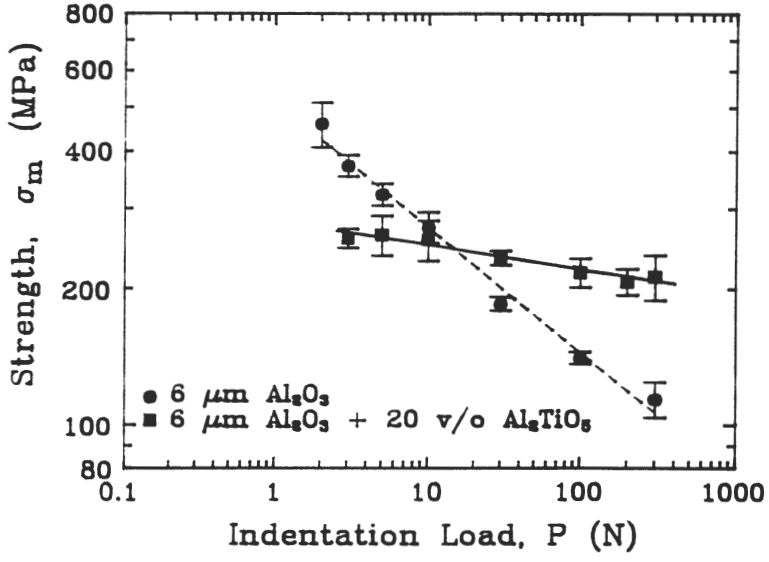

Figure 5 Plot of $\sigma_M(P)$ for Al_2O_3–Al_2TiO_5 composite and control Al_2O_3. The composite shows superior flaw tolerance.

We have shown that optimization of grain-localized crack bridging in Al_2O_3 can be achieved by incorporation of an Al_2TiO_5 second-phase, via enhancement of local TEA stresses. The attendant crack stabilization yields a composite that is highly damage resistant (fig. 3), with strong *T*-curve characteristics (fig. 4) and high flaw tolerance (fig. 5). With regard to the *T*-curve in fig. 4, scatter in the *in situ* data arises from uncertainties in crack-size measurements, and from crack-size variations in the crack-geometry and indentation coefficients ψ [14] and χ [15]. Slow crack growth can also lead to an underestimate of the toughness level [10]. The data range using indentation flaws is limited by the contact loads at which well-formed, dominant radial crack systems are obtainable. Notwithstanding these qualifications, the *in situ* technique presents itself as a powerful means of *T*-curve evaluation in the critical short-crack region that determines strength and other (e.g. wear) properties of structural ceramics; and, moreover, provides valuable information on the crack-microstructure interactions fundamentally responsible for the *T*-curve.

ACKNOWLEDGEMENTS

The authors acknowledge discussions with E.R. Fuller Jr. and N.P. Padture, and experimental assistance from J.L. Runyan. Funding was provided by the U.S. Air Force Office of Scientific Research and E.I. duPont de Nemours and Co. Inc.

REFERENCES

1. Y-W. Mai and B.R. Lawn, "Crack Stability and Toughness Characteristics in Brittle Materials," *Ann. Rev. Mater. Sci.* **16** 415-39 (1986).

2. R.W. Steinbrech and O. Shmenkel, "Crack Resistance Curves of Surface Cracks in Alumina," *J. Amer. Ceram. Soc.* **71**[5] C-271-73 (1988).

3. D.J. Green, R.H.J. Hannink and M.V. Swain, *Transformation Toughening of Ceramics*. CRC Press, Boca Raton, Florida, 1989.

4. A.G. Evans, "Perspective on the Development of High-Toughness Ceramics" *J. Amer. Ceram. Soc.* **73**[2] 187-206 (1990).

5. B.R. Lawn, *Fracture of Brittle Solids*, second edition. Cambridge University Press, Cambridge, UK, 1991.

6. R.F. Cook, C.J. Fairbanks, B.R. Lawn and Y-W. Mai, "Crack Resistance by Interfacial Bridging: Its Role in Determining Strength Characteristics," *J. Mater. Research* **2**[3] 345- 56 (1987).

7. S.J. Bennison and B.R. Lawn, "Role of Interfacial Grain-Bridging Sliding Friction in the Crack-Resistance and Strength Properties of Nontransforming Ceramics," *Acta Metall.* **37**[10] 2659-71 (1989).

8. J.L. Runyan and S.J. Bennison, "Fabrication of Flaw-Tolerant Aluminum-Titanate-Reinforced Alumina," *J. Europ. Ceram. Soc.* **7** 93-99 (1991).

9. S.J. Bennison, N.P. Padture, J.L. Runyan and B.R. Lawn, "Flaw-Insensitive Ceramics," *Philos. Mag. Letters* **64**[4] 191-95 (1991).

10. L.M. Braun, S.J. Bennison and B.R. Lawn, "Objective Evaluation of Short-Crack Toughness-Curves Using Indentation Flaws: Case Study on Alumina-Based Ceramics," Submitted *J. Amer. Ceram. Soc.*

11. E.C.M. Pennings and W. Grellner, "Precise Nondestructive Determination of the Density of Porous Ceramics," *J. Amer. Ceram. Soc.*, **72** [2] 1268-70 (1989).

12. J.C. Wurst and J.A. Nelson, "Lineal Intercept Technique for Measuring Grain Size in Two-Phase Polycrystalline Ceramics," *J. Amer. Ceram. Soc.,* **55** [2] 109 (1972).

13. N. Ramachandran and D.K. Shetty, "Rising Crack-Growth-Resistance (*R*-Curve) Behavior of Toughened Alumina and Silicon Nitride," *J. Amer. Ceram. Soc.* **74**[10] 2634-41 (1991).

14. S.M. Smith and R.O. Scattergood, "Crack Shape Effects in Fracture Toughness Measurements," *J. Am. Ceram. Soc.*, in press.

15. C-W. Li, D-J. Lee and S-C. Lui, "*R*-Curve Behavior and Strength of *In Situ* Reinforced Silicon Nitride with Different Microstructures," *J. Amer. Ceram. Soc.*, submitted.

16. D.B. Marshall, B.R. Lawn and P. Chantikul, "Residual Stress Effects in Sharp-Contact Cracking: II. Strength Degradation," *J. Mater. Sci.* **14**[9] 2225-35 (1979).

17. J. Rödel and S.J. Bennison, unpublished work.

18. P. Chantikul, S.J. Bennison and B.R. Lawn, "Role of Grain Size in the Strength and *R*-Curve Properties of Alumina," *J. Am. Ceram. Soc.* **73**[8] 2419-27 (1990).